Microwave Temperature Compensated Detector Design for Wide Dynamic Range Applications

Germán Torregrosa-Penalva, Alberto Asensio-López, Jaime Lluch-Ladrón de Guevara, and Francisco Javier Ortega-González

Departamento de Señales, Sistemas y Radiocomunicaciones.
ETSI Telecomunicación. Universidad Politécnica de Madrid.
Ciudad Universitaria, s/n. 28040 Madrid. SPAIN.
Phone: 34-91-3367358. Fax: 34-91-3367362.
Email: german@gmr.ssr.upm.es

Germán Torregrosa-Penalva, Alberto Asensio-López, and Jaime Lluch-Ladrón de Guevara are with the E.T.S.I. Telecomunicación, Universidad Politécnica de Madrid (G.M.R. of S.S.R.). Ciudad Universitaria, s/n. 28040 Madrid. SPAIN.

Francisco Javier Ortega-González, is with the E.U.I.T. Telecomunicación, Universidad Politécnica de Madrid.

Acknowledgements:

This work was supported by INDRA SISTEMAS and Project TIC-1999-1172-C02-01/02 of the National Board of Scientific and Technology Research (CIYCIT).

The authors would like to acknowledge José Luís Jiménez-Martín for valuable suggestions.

Microwave Temperature Compensated Detector Design for Wide Dynamic Range Applications

I. INTRODUCTION

Modern radar and communications systems usually include and make use of intelligent management of their transmitters output power. The main goals achievable through this function go from interference elimination in systems sharing the same covering range, to configuration of LPI (low probability of interception) systems, where a spatial management of the output transmitted power may even constitute a system requirement. Also, transmitters' reliability must be ensured through the use of power sensors to implement BITE (built in test equipment) functions. As a conclusion transmitters should include power detectors able of efficiently and precisely operating under wide power and temperature ranges.

This paper presents the key clues necessary for designing this kind of detectors. Fundamentals on RF detection, Schottky diode matching techniques, temperature compensation schemes and video output system configurations are reviewed. As an example, an X band detector design is presented which makes use of a low cost commercial packaged Schottky diode (MA4E2054 by MACOM). It achieves an RF input power range larger than 35.0dB and ±0.3dB peak error due to temperature changes within the range -25.0ºC to 85.0ºC. The detector's performance was tested and measured within a 10.0% bandwidth centered at 9.0GHz.

For temperature compensation purposes it will be demonstrated through simulation results that large signal operation of the nonlinear element is more suitable. Large signal operation though cannot be obtained for a wide range of RF input power

levels as desired, so small signal operation is also necessary if a dynamic range larger than 35.0 dB is desired. Small and large signal simulations were carried out making use of Advanced Design System (ADS) by Agilent Technologies.

Expressions to determine the optimum working point for small signal operation matching, temperature compensation effects and wide RF input dynamic range are also included.

II. RF DETECTION FUNDAMENTALS. SCHOTTKY BASED RF DETECTORS. SMALL SIGNAL OPERATION

Microwave detector diodes use the nonlinear junction resistance for their operation. If a sinusoidal RF input signal is assumed ($\Delta V = V_p \cos(\omega_c t)$), the current through the nonlinear element can be expressed using Taylor's expansion, [1] and [2], as shown in eq. 1.

$$i = i(V_0) + V_p \cos(\omega_c t)\left.\frac{di}{dv}\right|_{I_0} + \frac{V_p^2}{2}\cos^2(\omega_c t)\left.\frac{d^2 i}{dv^2}\right|_{I_0} \quad \textbf{(1)}$$

The DC component in eq. 1 can be expressed as shown in eq. 2,

$$I = i(V_0) + \frac{V_p}{4}\cdot\left.\frac{d^2 i}{dv^2}\right|_{I_0} \quad \textbf{(2)}$$

where $i(V_0)$ is the bias current term, and the second term is due to the presence of RF input signal and it depends on the RF power level through V_p.

The characteristics of the diode to be used in the proposed example are given in Table I. Figure 1 shows the packaged device equivalent circuit which includes two Schottky diodes.

Table I: MA4E2054 spice model parameters.

PARAMETER	VALUE	PARAMETER	VALUE
I_{sat} (μA)	3.0e-2	V_j (V)	0.40
R_s (Ω)	11.0	M	0.50
Cj(0) (pF)	0.10	EG (eV)	0.69
N	1.05	IBV (μA)	10.0
BV (V)	5.0	TT (sec)	0

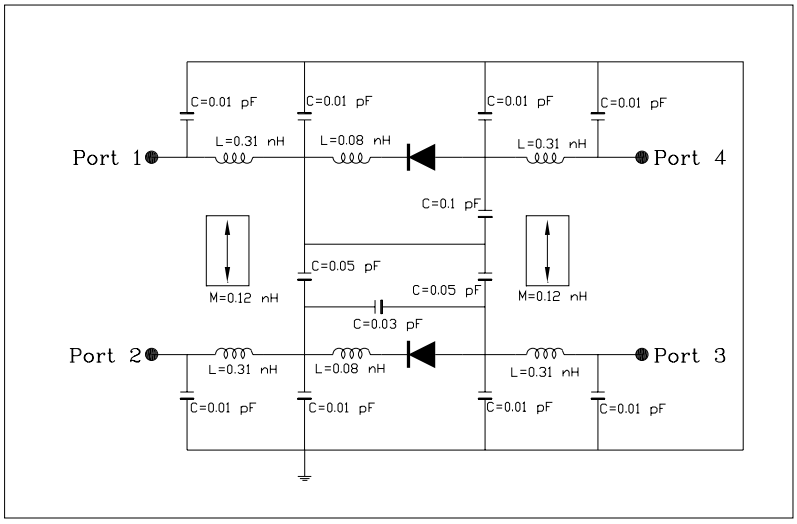

Figure 1: Diode pair MA4E2054 by MACOM.

The basic expression that relates the voltage drop across the diode and the current through its terminals for a Schottky diode is presented in eq. 3.

$$i = I_S\left(e^{\frac{e}{nkT}V_j} - 1\right) \tag{3}$$

The most commonly used and simplest small signal equivalent model for a Schottky diode is presented in fig. 2. Three basic elements are required to model the behavior of this device under small signal operation:

- **Junction resistance (R_j)**: it is the inverse of the I-V slope relationship and it can be expressed as

$$R_j = \left[\left.\frac{di}{dv_j}\right|_{I_0}\right]^{-1} = \left[\left.\frac{d}{dv_j}\left[I_S\left(e^{\alpha v_j} - 1\right)\right]\right|_{I_0}\right]^{-1} = (...) = \frac{nkT}{e(I_S + I_0)} \tag{4}$$

  where:

  - I_S is the saturation current.
  - I_0 is the DC current through the diode.

- **Series resistance (R_S)**: it represents ohmic contacts, substrate losses...
- **Junction capacitance (C_j)**: which depends on the voltage drop. C_j should be small enough so as not to shunt the RF current across the diode's resistance R_j. A parameter that allows the measurement of the device's efficiency is the cutoff frequency f_c defined as:

$$f_c = \frac{1}{2\pi C_j R_s} \tag{5}$$

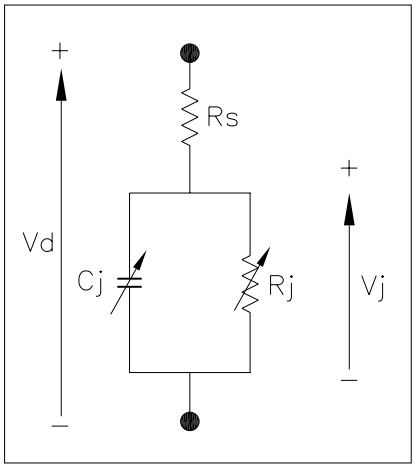

Figure 2: Schottky diode equivalent model.

III. DETECTION SCHEMES

III.I. Single diode detection configuration

The most common diode based detection scheme found in the bibliography is shown in fig. 3, [1], [2] and [3].

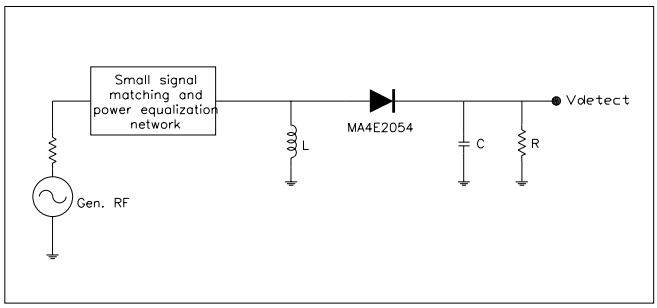

Figure 3: Basic RF detection scheme.

Figure 3 also shows the key elements of a conventional RF detector:

- **RF filtering and matching network. RF input power equalization**. It is important to notice at this point that input RF matching should be obtained not just for the whole working bandwidth, but also for the whole range of RF input power levels [4] (for large signal operation). In the case of this paper, as a large dynamic range (larger than 35.0dB) was desired, this feature was intelligently used as a way to make even larger the detector's dynamic range through the use of power equalization under large signal operation. The key idea is to prevent the diode from saturating at a rather low input signal power level. In order to do so the designed detector takes advantage of the fact that the behavior of the input matching network will depend on the input signal power level [5]. The detector is on purpose unmatched at high input power levels of the radiofrequency signal, thus extending the input power dynamic range as desired.

  Also the use of lumped components has been avoided as much as possible for low cost and mounting considerations. The input matching network was entirely designed making use of distributed elements.
- **RF choke**. It is the return path for the DC rectified component and behaves as an open circuit for the RF signal.
- **Schottky diode**. It is the nonlinear element where harmonically related components (as well as DC current) are generated from the RF signal.
- **Output capacitor**. It is necessary to avoid the presence of RF signals (the fundamental frequency and the generated harmonics) at the detector's video circuit through the use of a grounded capacitor.

- **Video circuit**. In the case of the simple scheme presented in figure (2) a single resistance.

The basic scheme shown in fig. 3 presents two main problems. The first one is the fact that detector RF performance is influenced by the value of the video output resistor [5]. The change of the output resistance in configuration of fig. 3 completely modifies the diode's biasing point for a specific RF input power level. It would be desirable to have both RF input detection stage and video voltage processing block well isolated, so that both can be modified without disturbing each other's behavior. In order to do so an operational amplifier was used (see fig. 4). With this new scheme the RF stage has at its output a shortcircuit at RF frequencies (due to the grounded output capacitor) and also a shortcircuit at the DC component (due to the operational amplifier virtual ground), thus making RF-video stages isolation complete.

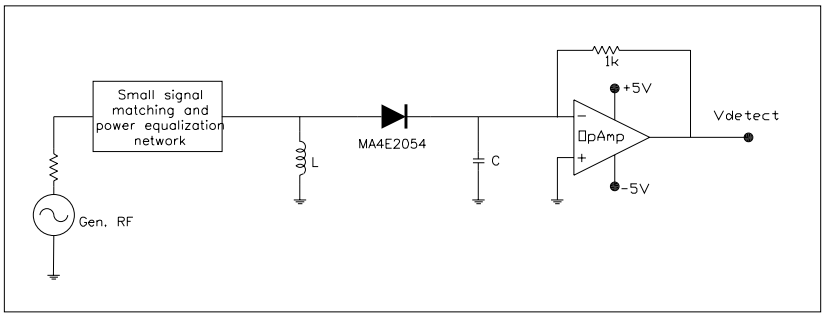

Figure 4: Basic RF detection scheme with op amp.

The second problem associated to the basic scheme of fig. 3 is the strong dependence of the detected current on temperature, especially at low RF input levels. If a large power range is needed over a wide working temperature range then this dependence must be eliminated. Both detected current and input matching depend on

the diode junction resistance (R_j) which at the same time depends on temperature. In order to study more precisely this dependence it is necessary to make use of large signal simulation tools. Large signal operation was simulated with the LSSP [6] circuit simulation block from ADS.

Figure 5 shows the simulated results obtained of the detected current in scheme of fig. 4 as a function of the RF input power level and temperature.

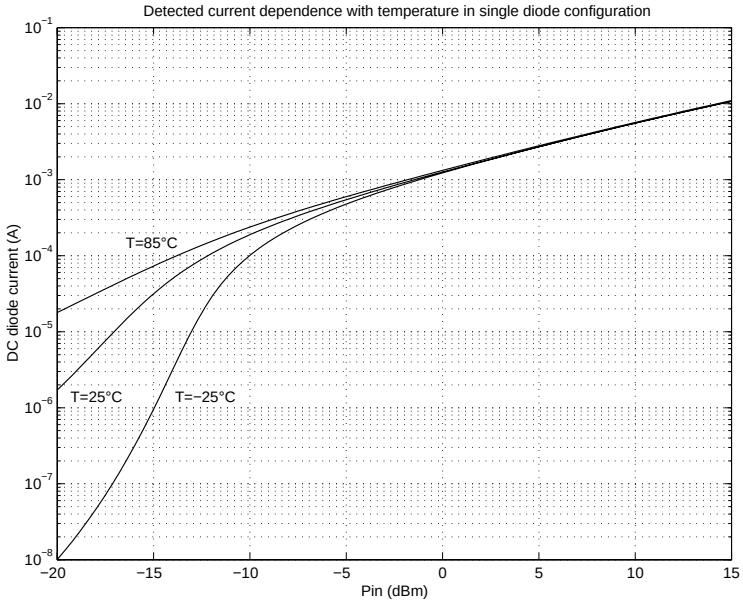

Figure 5: Detected current dependence with temperature.

Equation 6 shows the dependence of junction resistance with temperature for small signal operation.

$$R_j = \frac{nkT}{e\left(I_{sat} + I_{\det}\right)} \tag{6}$$

The temperature dependence of junction resistance is found to be due to two factors:

- Direct dependence with temperature.

- Dependence through saturation current as shown in eq. 7.

$$I_{sat} = I_{s0}\left(\frac{T}{T_0}\right)^{\frac{2}{n}} e^{\frac{-e\psi}{k}\left(\frac{1}{T}-\frac{1}{T_0}\right)} \quad \textbf{(7)}$$

The temperature dependence of the saturation current of the specific diode used in this design is shown in fig. 6.

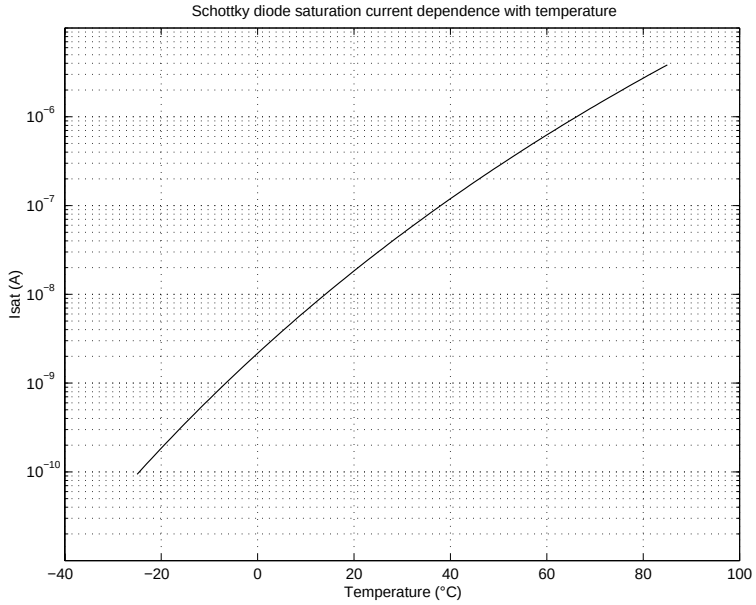

Figure 6: Saturation current dependence with temperature.

III.II. Diode Biasing

The solution given to the temperature dependence problem was the addition of bias current [1], which reduces both junction resistance (see fig. 8.a) and detection sensibility $K(^{mA}/_{\mu W})$ (see fig. 8.b) dependence with temperature, and also facilitates diode matching by reducing junction resistance.

The biasing network (see fig. 7) is formed by three simple elements:

- RF choke.
- Biasing resistance (R_{bias}).
- Biasing voltage (V_{bias}).

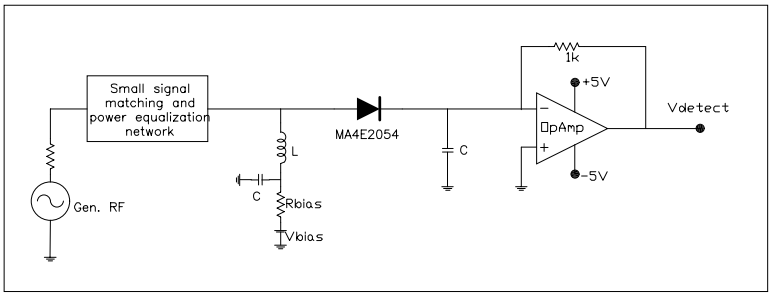

Figure 7: Single biased diode.

The reduction of junction resistance dependence with temperature can be easily demonstrated by the inclusion of the I_{bias} term in eq. 6.

$$R_j = \frac{nkT}{e\left(I_{sat} + I_{\det} + I_{bias}\right)} \tag{8}$$

In fact as ($I_{bias} >> I_{sat}$) R_j may be expressed as in eq. 9.

$$R_j = \frac{nkT}{e\left(I_{\det} + I_{bias}\right)} \tag{9}$$

Also including I_{bias} reduces direct dependence with temperature as shown in eq. 10.

$$\frac{dR_j}{dT} = \frac{nk}{e\left(I_{\det} + I_{bias}\right)} \tag{10}$$

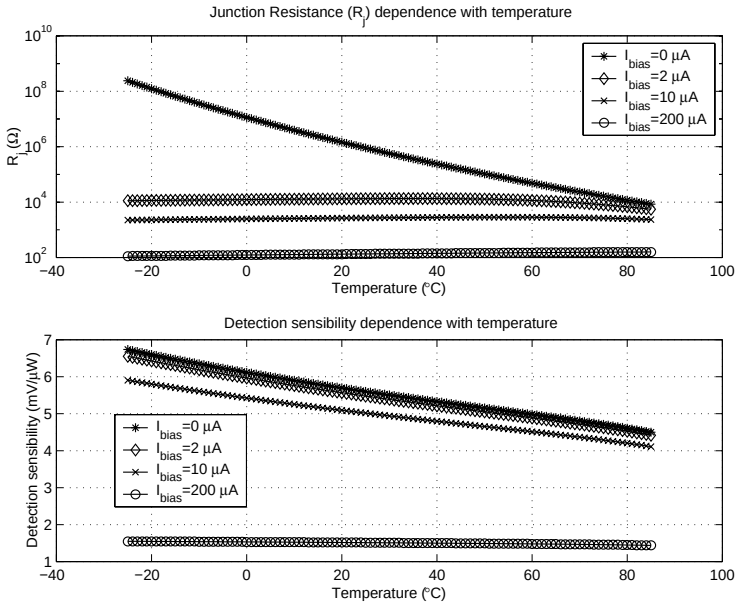

Figure 8: Junction resistance and detection sensibility dependence with temperature.

However the addition of I_{bias} introduces an offset term in the current flowing through the diode (I_{diode}) which may be expressed as

$$I_{diode} = I_{bias}(T) + I_{\det} + I_{sat} \cong I_{bias}(T) + I_{\det} = I_{bias}(T) + K(T) \cdot P_{in} \qquad \textbf{(11)}$$

where:

- $I_{bias}(T)$ is the biasing current which depends on temperature.
- K(T) is the detection sensibility ($^{mA}/_{\mu W}$) which depends on temperature.
- P_{in} is the RF input power level.

For temperature compensation it is necessary to eliminate $I_{bias}(T)$.

III.II. Two diode configuration

Elimination of $I_{bias}(T)$ is done by means of another diode biased at the same point as the first one [7]. The current trough this second diode is

$$I_{diode2} = I_{bias}(T) \tag{12}$$

Temperature compensation of the offset term is obtained if the difference between the current through both diodes is made.

With all these points in mind the final detector configuration is shown in figure 9.

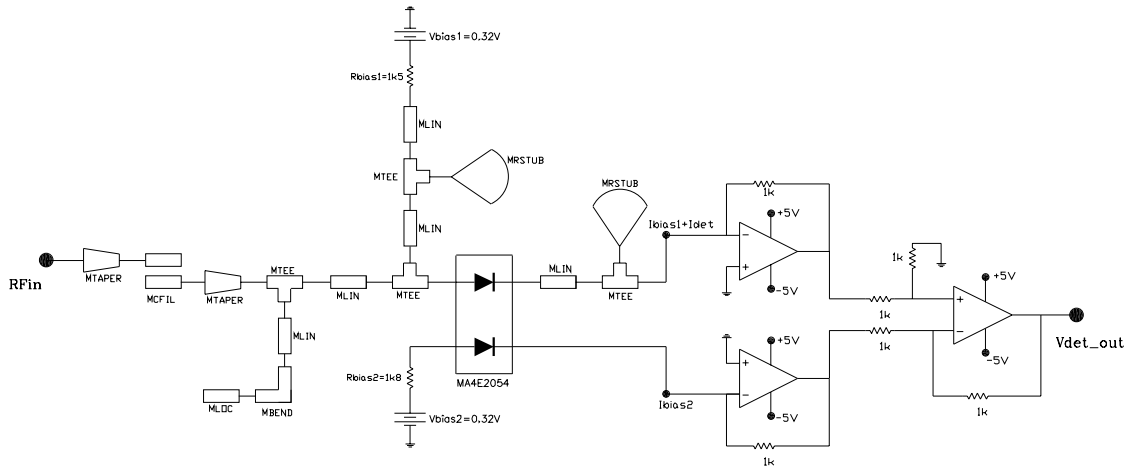

Figure 9: Final detector scheme.

Figure 10 shows the diode input matching as a function of the RF input power level.

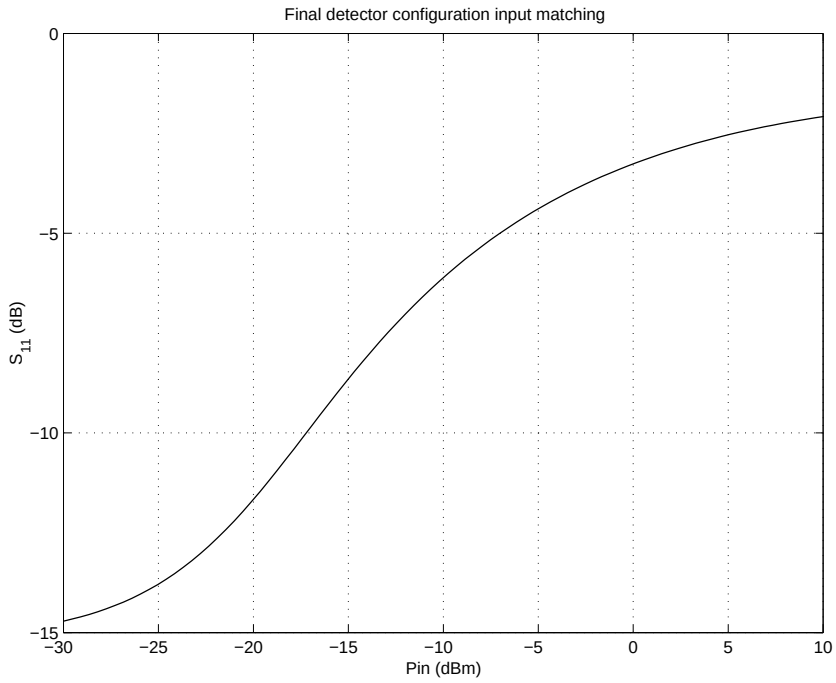

Figure 10: Input matching.

IV. RESULTS

Four different configurations are next presented to show the design process previously explained.

IV.I. Single diode detection scheme

First of all a single diode detector configuration was measured (fig. 4). The configuration shown in fig. 9 was mounted and measured but it just made use of a single diode in order to evaluate the need of the second one to compensate for the temperature dependence of the offset term.

The input matching network was designed following the ideas given in section III for large signal power equalization and small signal matching. The biasing parameters were chosen keeping in mind that:

- If V_{bias} is set too large then at low RF input power levels the detector will not have resolution at all because the current through the diode will be that of the biasing network.
- R_{bias} should be selected so that I_{bias} allows simple matching at the detector's input for small signal operation.

This considerations led to the selection of V_{bias}=0.32V and R_{bias}=820Ω.

The resulting measured response detected voltage versus RF input power is shown in fig. 11.a. In order to compare the improvements being obtained at each step of the designing process power detection errors were evaluated. The measured absolute error obtained in this configuration is shown in figure 11.b.

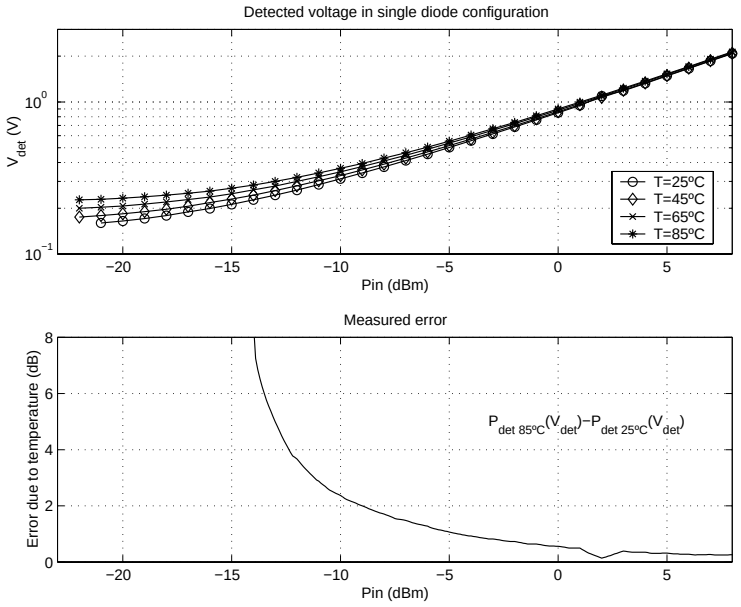

Figure 11: Detected measured voltage and measured error in single diode scheme.

Two main conclusions can be drawn at the sight of fig. 11:

- I_{bias} reduces significantly the detected voltage dependence on temperature changes.
- Detected voltage includes an important offset term due to bias current as shown in Table II that should be removed in order to improve the RF input dynamic range.

Table II: Offset term due to bias current.

TEMPERATURE (C)	OFFSET VOLTAGE (V)
25	0.137
45	0.161
65	0.188
85	0.213

IV.II. Two diode detection scheme. Same biasing network for both diodes

Results obtained from including this second diode (fig. 9) are given in fig. 12. Both diodes were biased making use of the same biasing network previously described in section IV.I.

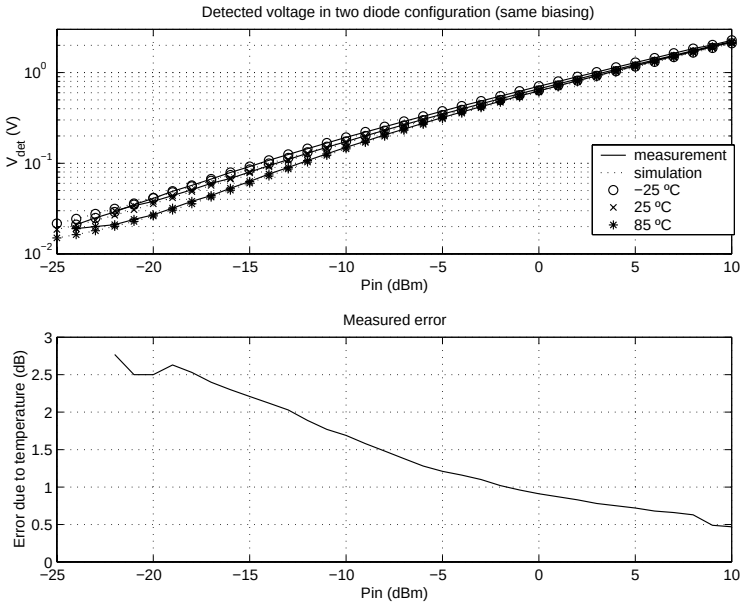

Figure 12: Detected voltage (measurements and simulations) and measured error in two-diode scheme. Same biasing for both diodes.

The offset term is eliminated trough the use of this second diode [7] and detectable power range has increased. Nevertheless, because of the use of low cost components for the video processing stage (low cost operational amplifiers) the offset term is not totally cancelled and detected power errors are still significant. Also, although errors due to temperature changes have significantly decreased, peak detection error at low input power levels is still unbearable for precision detection applications. This is due to the fact that the detection sensibility K(T) varies with temperature (eq. 11).

It is possible to correct the K(T) effect previously explained and further obtain substantial improvements with respect to the detector's behavior by making some small modifications.

As it has been said the current through each diode is given by eq. 12.

$$I_{diode1} = I_{bias1}(T) + K(T)P_{in}$$
$$I_{diode2} = I_{bias2}(T) \quad \textbf{(12)}$$

The key idea is to bring together the responses of the detected voltage for different temperatures at low RF input signal power levels, where errors mainly appear as shown in figs. 11 and 12. This could be done by slightly modifying the biasing parameters for the offset cancellation diode as it will be explained next.

For a given low input power level (P_{inlow}) and for the range of working temperatures [T_{max}, T_{min}], the detected current at the limits of the temperature range is given in each case by eq. 13.

$$I_{\det}(T_{min}) = I_{bias1}(T_{min}) + K(T_{min})P_{inlow} - I_{bias2}(T_{min})$$
$$I_{\det}(T_{max}) = I_{bias1}(T_{max}) + K(T_{max})P_{inlow} - I_{bias2}(T_{max}) \quad \textbf{(13)}$$

It would be desirable to have

$$I_{\det}(T_{min}) = I_{\det}(T_{max}) \quad \textbf{(14)}$$

so that no errors appear at P_{inlow}. Condition 14 may be accomplished by modifying I_{bias} of the diodes used in the design. If condition 14 is met then, as the rest of the detector's temperature responses are enclosed between those at T_{max} and T_{min}, reduction of errors is evident.

IV.III. Two diode detection scheme. Different biasing networks for each diode

In order to meet eq. 14 (for P_{inlow}=-22.0dBm) the biasing parameters for the first diode were maintained (V_{bias1}=0.32V and R_{bias1}=820Ω) while those of the second diode where changed to V_{bias2}=0.32V and R_{bias2}=910Ω.

Results obtained from performing this change are given in fig. 13.

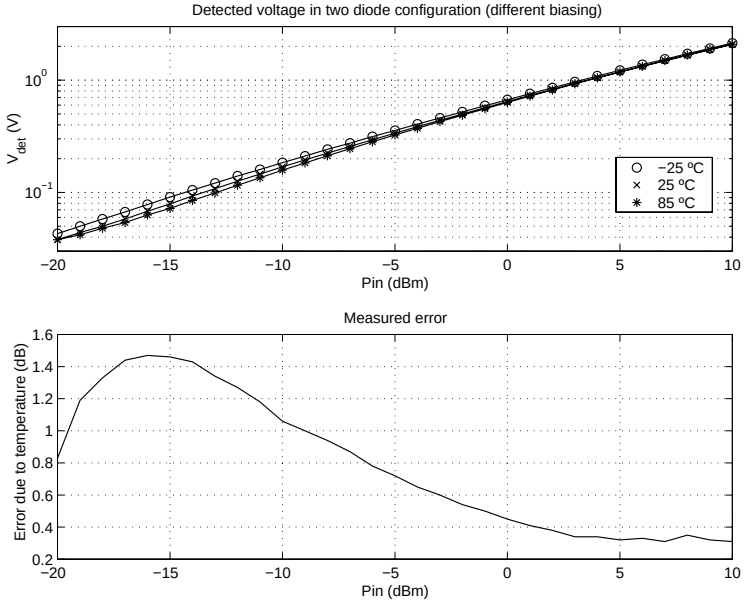

Figure 13: Detected measured voltage and measured error in two-diode scheme.

Error due to temperature has been almost eliminated through the use of different bias parameters for each diode.

IV.IV. Final detection scheme

When different biasing is used for each diode the output current is given by:

$$I_{\det}(T) = K(T)P_{in} + I_{bias1}(T) - I_{bias2}(T) = K(T)P_{in} + \Delta I_{bias}(T) \quad \textbf{(15)}$$

For low RF input signal power levels $\Delta I_{bias}(T)$ compensates the K(T) variations due to temperature drifts. In the case of fig. 13 for P_{in}=-15.0dBm the term $K(T)P_{in} >> \Delta I_{bias}(T)$ and thus compensation cannot occur.

If K(T) is made smaller through the use of a greater value of R_{bias1} then $\Delta I_{bias}(T)$ will be able to compensate for K(T) changes due to temperature for P_{in} values even larger than -15.0dBm.

R_{bias1} was chosen to be R_{bias1}=1.5KΩ and R_{bias2} was calculated to meet condition 14 (R_{bias2}=1.8K).

Results obtained from performing this change are given in fig. 14.

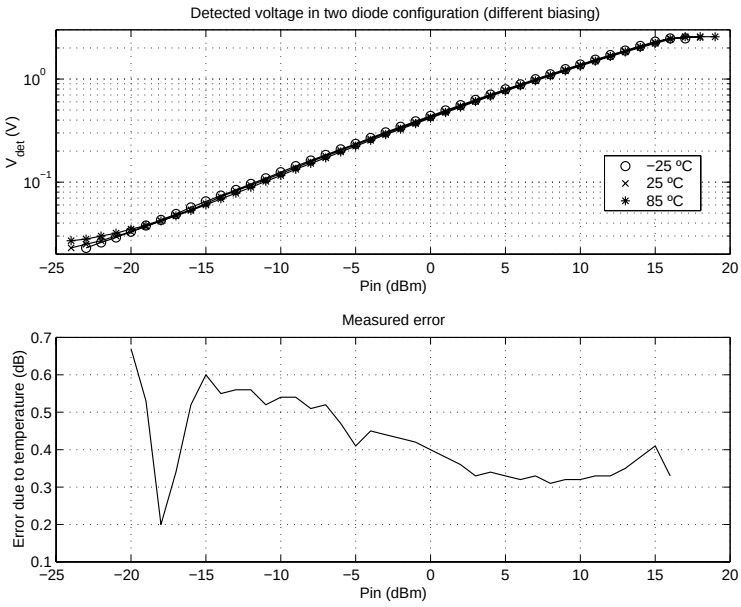

Figure 14: Detected measured voltage and measured error in two-diode scheme.

V. CONCLUSIONS

In this work basic design rules and key aspects for implementing power sensors operating under wide power and temperature ranges have been presented through different design examples. In each case experimental results and simulations have successfully confirmed the proposed step by step design technique.

REFERENCES

[1]I. Bahl and P. Bhartia. *Microwave Solid State Circuit Design*. John Wiley & Sons, 1988.

[2] D. M. Pozar. *Microwave Engineering*. John Wiley & Sons, 1998.

[3] "Schottky Barrier Video Detectors", *Application Note 923*, Hewlett Packard, 1986.

[4] "Impedance Matching Techniques for Mixers and Detectors", *Application Note 963*, Hewlett Packard, 1980.

[5] Harrison and Polozec. "Non-square Law Behaviour of Diode Detectors Analyzed by the Ritz-Galerkin Method", *IEEE Transactions on Microwave Theory and Techniques*, Vol. 42, No. 5, May 1994.

[6] "Diode Detector Simulation using Hewlett-Packard EESOF ADS Software", *Application Note 1156*, Hewlett Packard, 1998.

[7] R. J. Turner. "Schottky Diode Pair Makes an RF Detector Stable", *Electronics*, pp. 94-95, May 1974.